ISSUE: December 2022

Designing An Open-Source Power Inverter (Part 9): Magnetics For The Converter Control Power Supply

by Dennis Feucht, Innovatia Laboratories, Cayo, Belize

As we continue exploration of the Volksinverter design,[1-8] we pick up the discussion of the converter control power supply started in part 8. Located on the converter controller board, BCV401, this switching power supply uses hysteretic control to step down the 24-V source to 12-V for powering the control circuits (Fig. 1).

This part 9 reviews the design of the inductor for this power supply. This inductor design is not performance-driven, and this greatly simplifies the design, given here in a step-by-step *template* form so that both switching converter and inductor design can be applied more generally in other projects.

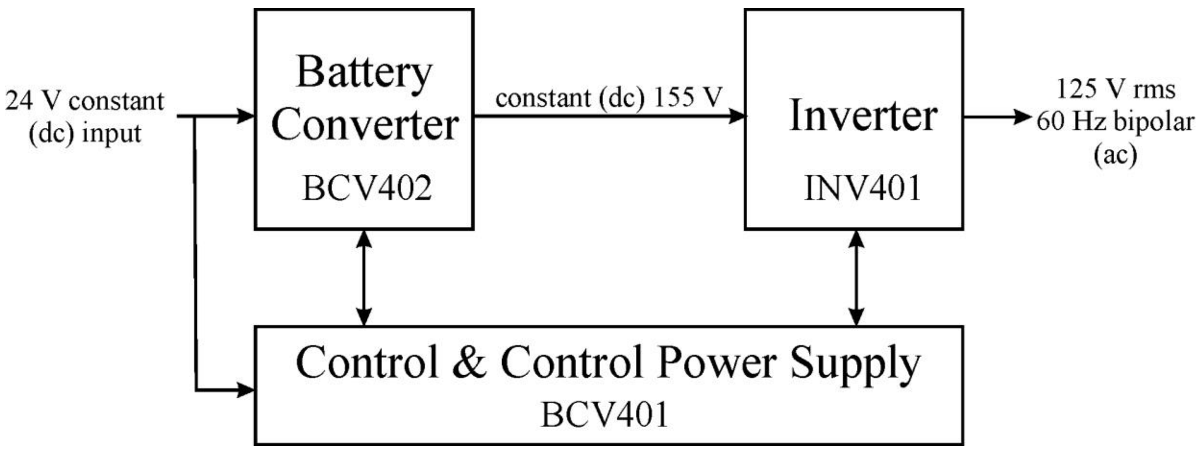

Fig. 1. The Volksinverter described in this series contains a separate stage—the control & control power supply stage, BCV401—for generating control signals and the +5-V and +12-V power rails for the control circuits. This part of the series discusses the design of the inductor required in the control power supply, which employs hysteretic control.

Magnetics Specifications From Circuit Design

The control power supply (PS) is a minimal-parts switching converter, repeated from part 8 as the circuit diagram of Fig. 2. The magnetic component is L1, the supply PWM-switch inductor.

The design begins with the converter control power supply specifications. The circuit diagram gives the major details of inductor construction. An optimizing design would include procedural details bypassed or shown to be avoidable in this design review. For undemanding performance, where highest power density or efficiency is not required, inductor design can be greatly simplified, as is demonstrated here.

The PS must operate over the input voltage range of the inverter, from

$$V_g \in [20\text{ V}, 25\text{ V}, 30\text{ V}]$$

with a corresponding power-transfer circuit duty-ratio of

$$D = \frac{V_o}{V_g} \in [0.625, 0.5, 0.416]\,;\;\; D' = 1 - \frac{V_o}{V_g} \Rightarrow D' \in [0.375, 0.5, 0.5833]$$

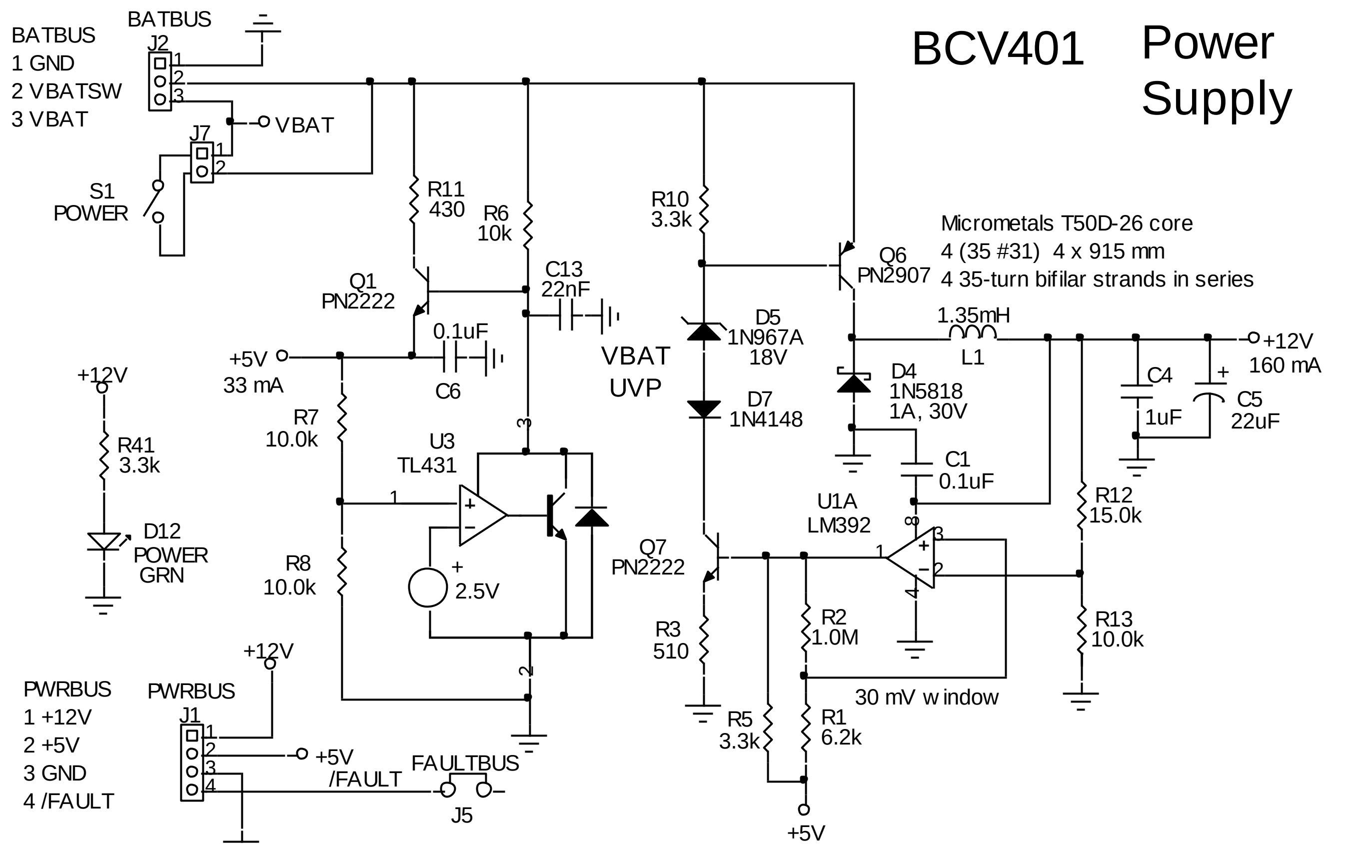

Fig. 2. Circuit diagram of the BCV401 power supply. It outputs to a four-pin power bus (PWRBUS) which includes the fault-bus line. The BATBUS connector brings in a nominal 24-V from the battery on VBAT which is switched by an optionally off-board power switch, S1. The L1 inductor winding is four strands of twisted #31 AWG wire 915 mm long. The four strands are connected in series external to the winding.

The order of values in the *D* and *D'* ranges correspond to those in V_g. Maximum average output and inductor current is

$$\bar{i}_o = \bar{i}_L = 0.16\text{ A}$$

Maximum output voltage ripple is specified to be ΔV_o = 75 mV with a design average V_o = 12.5 V. Then

$$\frac{V_o}{\hat{v}_{O\sim}} = \frac{V_o}{\Delta v_O / 2} = \frac{12.5\text{ V}}{75\text{ mV/2}} = 333.3$$

From the wire table,[9] the rated output current of $I_o = \bar{i}_o = \bar{i}_L$ = 0.16 A corresponds to a wire size of #31 AWG having an ampacity of I_{max} = 0.187 A. The CCM hysteretic controller has constant-Δv_O with output frequencies derived in part 8 and calculated from

$$f_s = \frac{1}{2 \cdot \tau_n} \cdot \sqrt{D' \cdot \frac{V_o}{\hat{v}_{O\sim}}}\ ,\ \tau_n = \sqrt{L \cdot C_o} \quad \Rightarrow \frac{f_s}{f_n} = \pi \cdot \sqrt{D' \cdot \frac{V_o}{\hat{v}_{O\sim}}} = \sqrt{D'} \cdot (57.35)$$

D' varies with V_g, resulting in the following table of switching to resonant frequency ratios over the V_g range.

Table. Switching-to-resonant frequency ratio versus battery converter input voltage.

V_g, V	f_s/f_n
20	35.12
25	40.56
30	43.80

The frequency values assume no loop delay in the hysteretic controller and will be numerically somewhat high. The design values are taken to be

$$f_s \in [35\text{ kHz}, 40\text{ kHz}, 45\text{ kHz}]$$

Solving for

$$f_n = \frac{1}{2 \cdot \pi \cdot \tau_n} \Rightarrow f_n = \frac{1}{2 \cdot \pi \cdot \sqrt{(1.35\text{ mH}) \cdot (18\,\mu\text{F})}} = 1021\text{ Hz}$$

Inductor Calculations

The prototype circuit-board layout is shown in Fig. 3. The layout pattern for toroid inductor L1, denoted by the circle (erroneously marked as "135 µH" within it), has four vertically-aligned pads each on the left and right sides for connection from two windings that connect on the top (red-trace) side of the board to form the complete inductor.

This slight complication of connecting the four wire strands in series simplifies inductor construction in that two windings in parallel with one-fourth the turns results in the same inductance but reduces winding effort with fewer turns. The unsaturated inductance is expected to be about

$$L_0 = \frac{\tau_n^2}{C_o} = \frac{1}{(2 \cdot \pi \cdot f_n)^2 \cdot C_o} = 1.41\text{ mH}$$

By oversizing the small core, it is easier to wind and also saturates less so that $k_{sat} \approx 1$. A half-inch-diameter toroid fits this board part pattern and at least three toroids of that size with differing heights are available, offering some freedom of core choice in design.

From the wire table, a single strand of #31 round Cu wire has an insulated (heavy) radius of r_{cw} = 0.134 mm, an area with packing factor included of A_{cwp} = 0.107 mm^2 and a frequency of $f(r_c = \delta) = f_\delta$ = 409 kHz at which the conductive radius $r_c = \delta(f)$, the eddy-current *skin depth*

$$\delta(f) = \frac{73.5\text{ mm}}{\sqrt{f/\text{Hz}}}\text{, Cu, 80 °C}$$

Wire radius r_c can be expressed in units of skin depth (in what is otherwise called the *penetration ratio*) as

$$\xi_r = \frac{r_c}{\delta}$$

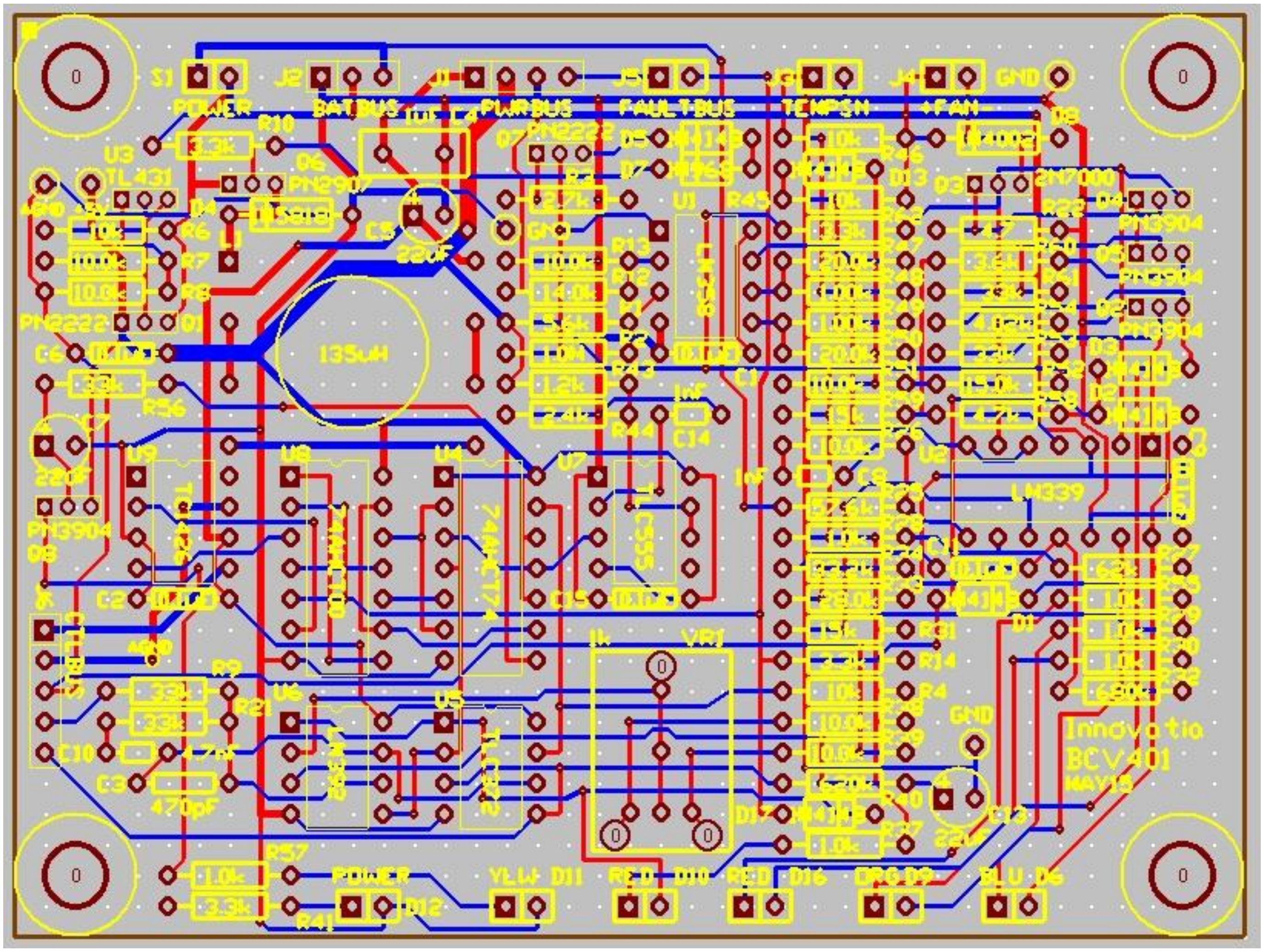

Fig. 3. Layout of an early BCV401 converter control etched-circuit-board (ECB). The board is 3 × 4 in. with four #8 mounting holes, 0.2 × 0.2 in. from the corners. Through-hole components are used for ease of prototype probing and replacement. Interface board connectors are at the top and bottom of the ECB. Ground (GND) test points are for ground clips.

Then $f_\delta = f(\xi_r = 1)$. At $\xi_r = 1$, the constant-wire-size eddy current resistance ratio $F_R(\xi_r \le 1) \approx 1$ and the effect of eddy current on winding resistance is negligible. At the limits of the PS's switching frequency range,

$$\xi_r(35\,\text{kHz}) = \sqrt{\frac{f}{f_\delta}} = \sqrt{\frac{35\,\text{kHz}}{409\,\text{kHz}}} \approx 0.293\ ;\ \xi_r(45\,\text{kHz}) = \sqrt{\frac{f}{f_\delta}} = \sqrt{\frac{45\,\text{kHz}}{409\,\text{kHz}}} \approx 0.332$$

Both are significantly less than one and therefore eddy-current loss can be ignored in this design.

From the wire table, #31 AWG wire has an *ampacity* of rms I_{max} = 187 mA and exceeds the design maximum output current of 0.16 A. (Ampacity of the wire also varies with core size and is even smaller with small cores.) Wire cross-sectional area including packing factor is A_{cwp} = 0.107 mm^2 and insulated radius r_{cw} = 0.138 mm.

To minimize turns, an Fe-pwd core of high field inductance was chosen: the T50D-26. Its design parameters, taken from the Micrometals core catalog, are

Winding area = A_w = 46.6 mm^2

Inside radius = r_i = 3.85 mm

Average core radius (to middle of core) = $\bar{r}$ = 5.10 mm

Core width = w = 2.5 mm

Core height = h = 9.53 mm

Field inductance (per-turn-squared inductance) = $\mathcal{L}_0$ = 72 nH

Then the number of turns

$$N = \sqrt{\frac{L_0}{\mathcal{L}_0}} = \sqrt{\frac{1.41\,\text{mH}}{72\,\text{nH}}} = 140 = 4 \cdot 35$$

Thus 35 turns of four strands of #31 wire (#31 × 4) connected in series on the circuit-board gives 140 turns and

$$L_0 = N^2 \cdot \mathcal{L}_0 = (140)^2 \cdot (72\,\text{nH}) = 1.41\,\text{mH}$$

The maximum field current Ni = (140)·(0.16 A) = 22.4 A. For the T50D-26 core, a field current of 75 A has k_{sat} = 0.7. At 22.4 A, $k_{sat} \approx 0.91$, which represents negligible saturation for which

$$L = (0.91)\cdot\mathcal{L}_0 = (0.91)\cdot(1.41\text{ mH}) = 1.28\text{ mH}$$

Thus, 1.35 mH is a mid-scale value of L. A smaller core such as a T50B-26 might have been chosen instead, but a T50D is not large or costly and is a useful size to have in stock for control supplies in other applications.

Next, the winding area is $A_{ww} = N \cdot A_{cwp}$ = (140)·(0.107 mm^2) = 15 mm^2. Then the winding window fraction is $k_{ww} = A_{ww}/A_w$ = 0.32, where A_{ww} is the winding area and A_w is the core window area. This is an easy core to wind because only about a third of the winding window is occupied. This leaves adequate open space for threading the final turns through the core center.

Core and winding losses are not significant and are avoided for this low-power design. A more exacting design would result in the choice of a smaller core with higher transfer-power density and also higher loss density. The difference is not significant for this application and its design is much less demanding. (It prepares the reader with a procedural overview for the more involved power inductor design in the BCV402 battery converter.)

Determining Wire Length

The most intensive calculation is that of winding length. For other types of cores, it is possible to wind them from a wire or bundle spool and then cut when the required turns have been added to the core. Toroids are an exception in that the entire winding length must go through the center of the core for each turn, and this requires that the winding be cut to length before winding onto the core.

An accurate formula exists for winding length.[10, 11] The expressions used in the formula are constructed as follows. They can be stored in a memory calculator in the designated locations, as numbered, and at least four digits of accuracy should be retained.

1. Maximum number of layers of round wire = $\hat{M} = \dfrac{r_i}{(1.866)\cdot r_{cw}} = \dfrac{3.85\,\text{mm}}{(1.866)\cdot(0.134\,\text{mm})} = 15.40$

2. Maximum number of turns that fit in window = $N_w = \pi \cdot M^2$ = 744.8

3. Number of layers = $M = \hat{M} \cdot (1 - N / N_w)$ = 1.522

4. Store $h + w$ = 12.03 mm

5. Store r_{cw} = 0.134 mm.

The calculator memory locations now contain the numbers for the winding-length calculation:

$$l_w = 2 \cdot \pi \cdot M \cdot [(2 \cdot (h + w) + 8 \cdot M \cdot r_{cw}) \cdot (\hat{M} - M/2) + \tfrac{4}{3} \cdot (1 - M^2) \cdot r_{cw} + \bar{r}] = 36.43 \text{ cm} = 4 \times 91.1 \text{ cm}$$

Add about 2 cm per end for lead length, and the construction length is

$$l_w = 4 \times 95 \text{ cm}$$

This is a bundle of four strands of #31 AWG wire 95 cm long, twisted together. About one twist per centimeter of bundle length is recommended. Twisting strands into a bundle reduces bundle length slightly from the straight-wire strand length. (The derived formulas for how much, along with many other more refined design details are found in reference [10] and in previous *How2Power Today* articles such as the derivation of l_w in reference [11].)

If the same design exercise as for the T50D-26 core were carried out for the T50B-26 core, which differs in its core height as h = 6.35 mm and field inductance, $\mathcal{L}_0$ = 43.5 nH, then the following values would result:

N = 180 = 4 × 45 turns

k_{ww} = 0.413 (also not difficult to wind)

Field current = $N\bar{i}$ = 28.8 A ⇒ $k_{sat} \approx 1$ (also not much core saturation)

$\hat{M}$ = 15.40 ; N_w = 744.8 ; M = 1.522 ; $h + w$ = 8.85 mm ; $\bar{r}$ = 2.50 mm ⇒ l_w = 275.3 mm = 4 × 68.9 cm → 4 × 74 cm

The T50B-26 core size might even be reduced further in height to the T50-26 h = 4.83 mm. However, by shrinking core volume, height decreases, field inductance $\mathcal{L}_0$ decreases (to 33 nH), turns increase, and k_{ww} increases so that winding construction becomes more difficult.

This exercise for simple design of undemanding performance from an inductor shows how easy it is to design toroid inductors for PWM-switch power-transfer circuit applications. (I suspect that many inductors in products have been designed in this way.) Higher-power transfer circuits generally require more optimal design, but for low-power switching supplies, simplicity and ease of magnetics construction is often the driving parameter.

References

1. "Designing An Open-Source Power Inverter (Part 1): Goals And Specifications" by Dennis Feucht, How2Power Today, May 2021.
2. "Designing An Open-Source Power Inverter (Part 2): Waveshape Selection" by Dennis Feucht, How2Power Today, September 2021.
3. "Designing An Open-Source Power Inverter (Part 3): Power-Transfer Circuit Options" by Dennis Feucht, How2Power Today, April 2022.
4. "Designing An Open-Source Power Inverter (Part 4): The Optimal Power-Line Waveshape" by Dennis Feucht, How2Power Today, May 2022.

5. "Designing An Open-Source Power Inverter (Part 5): Kilowatt Inverter Circuit Design" by Dennis Feucht, How2Power Today, July 2022.
6. "Designing An Open-Source Power Inverter (Part 6): Kilowatt Inverter Control Circuits" by Dennis Feucht, How2Power Today, August 2022.
7. "Designing An Open-Source Power Inverter (Part 7): Kilowatt Inverter Magnetics" by Dennis Feucht, How2Power Today, September 2022.
8. "Designing An Open-Source Power Inverter (Part 8): Converter Control Power Supply" by Dennis Feucht, How2Power Today, November 2022.
9. *Power Magnetics Design Optimization*, D. Feucht, Innovatia, page 108, or any manufacturer wire data.
10. *Power Magnetics Design Optimization*, D. Feucht, Innovatia, pages 116 - 121.
11. "How To Calculate Toroid Winding Length" by Dennis Feucht, How2Power Today, September 2013.

About The Author

Dennis Feucht has been involved in power electronics for 40 years, designing motor-drives and power converters. He has an instrument background from Tektronix, where he designed test and measurement equipment and did research in Tek Labs. He has lately been working on projects in theoretical magnetics and power converter research.

For further reading on inverter design, see the How2Power Design Guide, locate the Power Supply Function category and select "DC-AC power inverters."